IEEE Transactions on Nuclear Science, Vol. NS-30, No. 4, August 1983

ANTIPROTON YIELD OPTIMIZATION IN THE CERN ANTIPROTON ACCUMULATOR

C.D. Johnson
CERN, Geneva, Switzerland

Summary

The setting-up and optimization of antiprotons injected into the Antiproton Accumulator was initially based upon the measurement of circulating antiprotons by integration of their Schottky signals. This has now been supplemented by amplitude distribution measurements using an internal target. Also, the more readily detectable pions, muons and electrons, injected along with the antiprotons, give information on machine aperture and orbits, which can serve as a monitor of injection conditions during antiproton stacking.

Introduction

During the early running-in of the AA we were somewhat handicapped by a lack of diagnostics for use when optimizing antiproton yield. This could be accurately measured on a pulse to pulse basis by integrating the signal from a longitudinal Schottky pick-up. The basic measurement took about 30 s but a set of values averaged and corrected for zero drift required 5 to 10 min of machine time. Each one of the injection parameters was individually set to give maximum yield, and this was a fairly lengthy business. For example: a systematic optimization of yield versus injection line steering, including injection kicker and septum strengths, or a complete scan of yield versus aperture in both planes could each take the best part of an eight-hour shift.

The means by which we have been able to speed up this process are described here together with some hints that we have gleaned on the absolute yields and the problems of extending the performance of the AA towards higher antiproton intensities.

Techniques and Methods

Schottky Yield Measurement

The longitudinal Schottky noise spectrum in a chosen harmonic band of the circulating antiproton signal, after subtraction of amplifier noise is squared and integrated to give a number proportional to the circulating antiproton current. The constant of proportionality is found by cross calibration against a d.c. current transformer using more intense beams of protons or stacked antiprotons and calibrated signal attenuators[1]. This remains our standard yield measuring technique and with careful use can give a precision of $\pm 10^5$ $\bar{p}$, i.e. 2% of our full-aperture yield.

Reverse Ejection

Initial setting up of the antiproton injection line is done with protons at 3.5 GeV/c injected into the AA from the CPS in the reverse direction along the antiproton transfer line. These protons are then ejected from the ejection orbit backwards along the antiproton injection line up to the production target. So-called reverse ejection[2] has already greatly improved the initial setting-up procedure since the various scintillator screens in the injection line, unusable during antiproton injection, can be employed to adjust steering magnets and check alignment of quadrupoles.

Beam Scrapers and Scintillation Counters

The AA is equipped with two sets of internal beam scrapers: one in a zero dispersion region, the other at a place where the momentum dispersion is large. Simple arrays of scintillation counters fed into multi-channel scalers monitor the secondary radiation as these scrapers are driven at constant speed through the injected beam, giving antiproton betatron amplitude distributions at the zero dispersion scraper and information on the momentum distribution at the other scraper position. Also, these counters are calibrated against the Schottky yield system and at higher beam intensities against the d.c. circulating current transformer and so allow antiproton intensity measurements over a large dynamic range.

Momentum selection can be achieved by shaving the injected antiprotons with the scrapers in the dispersive region.

Pion, Electron and Muon Loss Signals

With each antiproton accepted into the AA there are about 300 negative pions and roughly half that number of electrons. The pions decay with a time constant of 680 ns (close to the revolution period). 95% of the resulting muons are lost from the machine. The remainder circulate and in turn decay with a time constant of 73 μs. The circulating electrons lose by synchrotron radiation 1.8 MeV per turn. As the total energy spread on the injection orbit is 70 MeV they are all lost after 40 turns or 22 μs. The radiation loss signals during the interval from 3 μs until 22 μs after injection are dominated by these electron losses.

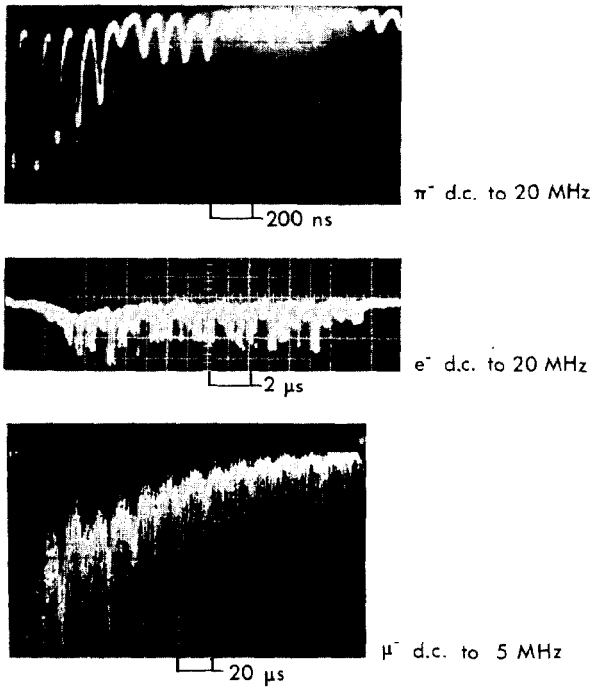

Fig. 1 - Pion decay, electron loss and muon decay signals after injection into the AA.

Pion decays are monitored by a Cerenkov counter tangential to the AA ring, the electron losses and muon decays by a set of 3 electron shower counters of the type used by Bailey et al.[3]. These are placed downstream from the pre-cooling shutters, which separate the pre-cooling and stack orbits in dispersive regions. Although the muon decay signal is independent of azimuthal position, the electron losses are localised at these shutters

0018-9499/83/0800-2821$01.00©1983 IEEE

since they are the first obstacles encountered by the spiralling electrons. The loss signal is naturally modulated at the bunch and revolution frequencies (9.5 and 1.85 MHz), in addition there is often an amplitude modulation at 510 kHz corresponding to coherent betatron oscillations, which modify the steady rate at which the electrons would otherwise reach the shutters.

After the electrons have gone away the muon decay signal can be observed. It has the characteristic form of an exponential decay modulated at the muon precession frequency (74 kHz in the AA). Examples of the pion, electron and muon loss signals are shown in Fig. 1.

Digital Filtering

The loss signals, in particular the electron signal, are sampled on each machine cycle by a 100 MHz CAMAC waveform digitizer. The sampling period is chosen to be 8 times the betatron oscillation period so that the 8th harmonic coefficients of the Discrete Fourier Transform, DFT, are a measure of the coherent oscillation amplitude and phase. The zero harmonic coefficient, the integral of the waveform, is proportional to the electron beam intensity and, as Q_h in the AA region is close to 2.265, the 30th coefficients give the modulation amplitude at the revolution frequency. In practice the sample period is adjusted to give the best resolution of the two frequencies and only the Fourier coefficients of interest need be evaluated.

Integrated Microcomputer System

Control and acquisition of the counter instrumentation together with acquisition of the scraper positions and the proton intensity on the production target are integrated into an autonomous microcomputer controlled CAMAC system with a simple link for the transfer of reduced data to the CPS Control Computer. The microcomputer, an LRS 3500, is programmed in compiled BASIC whith subroutines linked from a FORTRAN library. This on-line workstation includes a bit-slice processor for fast digital filtering and an interactive graphics facility for local data manipulation. Considerable use has been made of the latter to reconstruct calibrated antiproton beam profiles from the scraper measurements.

Yield Optimization

Electron Yield

The pion, electron and muon loss signals, integrated over various time windows, have been compared to simultaneous antiproton yields measured by the Schottky method during long periods of AA machine experiment and operation. Under stable machine conditions the integrated electron signal turns out to be well correlated to the Schottky yield and it suffers less from short-term drift. With the appropriate calibration it is used as a monitor of the pulse-to-pulse yield during an antiproton accumulation and stacking. It also serves as a means for quickly checking machine parameters during operation or experiment, usually peaking at the same settings that give maximum antiproton yield.

The pion signal, just visible on a fast circulating beam transformer, and the muon decay have also been employed but found to be less useful than the electrons, although the muon decay signal can give information on resonant losses during the interval from 25 μs to 250 μs after injection.

Electron coherent Oscillations

Electron loss signals in the band from d.c. to 2 MHz are shown in Fig. 2. Betatron oscillations, clearly visible in Fig. 2a are reduced by adjusting the injection septum magnet. The best setting is shown in Fig. 2b. Below each photograph is the corresponding DFT.

An experimental curve relating the magnitude of the 8th coefficient to the antiproton yield (Fig. 3) shows quite good agreement between minimum electron coherent oscillations and maximum antiproton yield. This seems to hold over all operational conditions.

A second pair of photographs, Figs. 4a and 4b show the reduction in coherent oscillations after re-steering the proton beam horizontally by 1 mm at the production target.

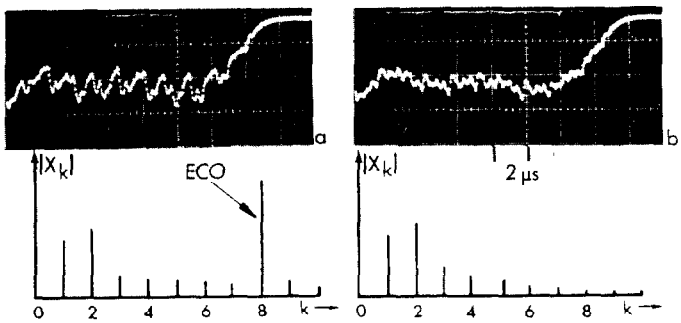

Fig. 2 - Electron loss signals (bandwidth d.c. to 2 MHz) and corresponding DFTs.

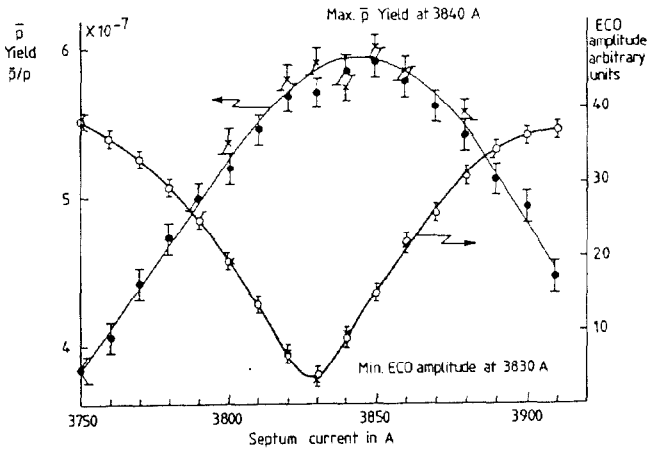

Fig. 3 - Antiproton yield and electron coherent oscillation amplitude (ECO) versus septum current.

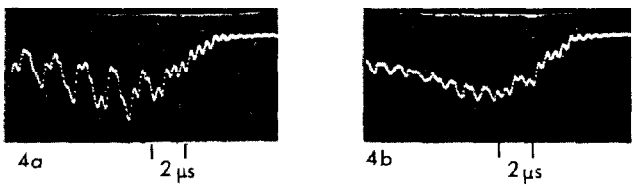

Fig. 4 - Electron loss signals before and after steering the proton beam on the production target.

Injection Timing

This is adjusted by minimizing the 9.5 MHz component of the electron loss signal, as illustrated in Fig. 5.

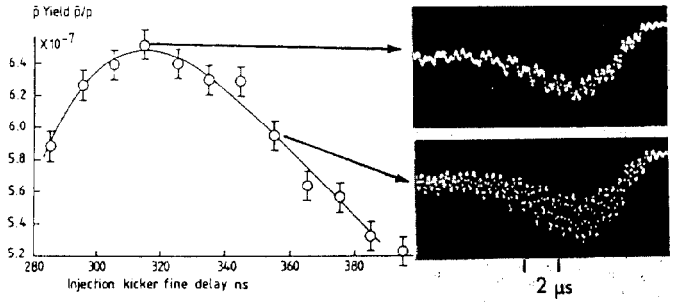

Fig. 5 - Antiproton yield versus injection timing fine delay. Electron loss signals at two settings.

Operational Procedure

Our method for finding the correct injection settinngs is to select the best kicker voltage by reverse ejection and then to minimize the coherent oscillations by varying injection line steering and injection septum strength. The injection timing is optimised and then the coherent oscillations are verified again. Yield measurements are only used as a final check on performance. Note that after selection of the kicker strength the remaining adjustments can be performed during antiproton stacking.

Transverse Antiproton Distributions

Beams of more or less uniform transverse phase-space density injected without loss into a machine with a rectangular aperture like the AA would be expected to have projected amplitude distributions of triangular shape. Known effects such as the fall-off in yield with laboratory production angle, antiproton absorption and scattering in the target, optics of the focusing horn just after the target, and the reduction in AA acceptance at the extreme momentum limits distort the shape to that shown as a broken line in Fig. 6.

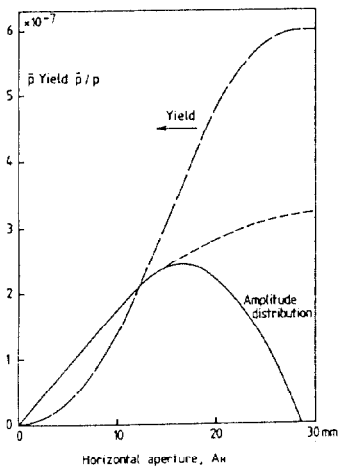

Fig. 6

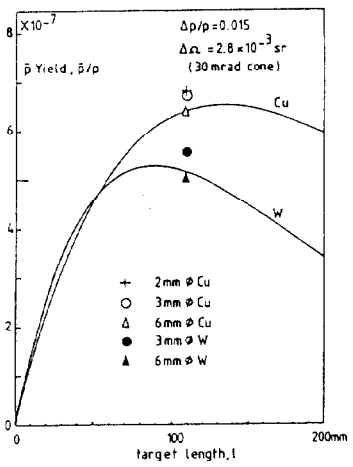

Fig. 7

In the AA, measured distributions peak at just over half of the maximum amplitude. Moreover, if the outer antiprotons are scraped away to leave only the inner core, which does have uniform phase-space density, all attempts to put particles out at large amplitudes, by kicking the scraped beam, result in renewed depletion in the outer regions of the aperture. We are presently trying to understand and correct this "soft" aperture limit. Linear coupling does not appear to be a sufficient explanation, and in any case this has already been compensated by a skew quadrupole. Some residual coupling between horizontal and vertical planes can nevertheless be demonstrated by kicking a vertically scraped beam horizontally and looking at the subsequent vertical distribution. This is always considerably enlarged by an amount proportional to the height before the kick.

Target Material

One consequence of the preponderance of low amplitude antiprotons is that the yield equation (1), which ignores particles escaping from the sides of the target, is a good approximation.

$$N_{\bar{p}} = W(p,\theta) \cdot \frac{p^2}{2E} \cdot \Delta p \cdot \Delta\Omega \cdot \frac{e^{-\ell/\lambda_p} - e^{-\ell/\lambda_{\bar{p}}}}{\lambda_p/\lambda_{\bar{p}} - 1} \qquad (1)$$

where $W(p,\theta)$ is the invariant production density, p the lab. momentum, E the total energy, Ω the lab. solid angle, and λ_p, $\lambda_{\bar{p}}$ the proton and antiproton absorption lengths, ℓ the target length.

Yield from copper and tungsten target for AA parameters using equation (1) are plotted in Fig. 7 together with measured values for 110 mm long targets of various diameters[4]. The curves have been normalised to the yield for the 6 mm diameter Cu target, which should give the best agreement with (1). The values of $W(p,\theta)$ are those given by Eichtein et al.[5]. The measured yield from 6 mm diameter tungsten is close to that given by (1). Our yield record is at present jointly held by 2 mm and 3 mm diameter Cu targets.

Conclusion

The maximum AA yield, which we now usually achieve within one shift of machine setting-up, at low acceptance corresponds to 70% of the AA Design Report estimates. This points to antiproton production densities somewhat higher than those reported by Eichten et al., which is consistent with the fit to data from different experiments given by Hojvat and Van Ginneken[6]. At full aperture we still lack a factor 2 in yield due to losses at large amplitudes.

Acknowledgements

The help of the AA Operations crew, the advice and support given by R. Billinge, V. Chohan, T. Dorenbos, E. Jones, S. van der Meer, T.R. Sherwood and E.J. Wilson and the technical assistance of M. Frauchiger is gratefully acknowledged.

References

1. W. Schnell, Schottky Diagnostics for Coasting Beams, CERN 77-13, 1977.

2. R. Billinge, T.R. Sherwood, (unpublished).

3. J. Bailay et al., CERN Muon Storage Ring, Nucl. Phys. B150:1, 1979.

4. C.D. Johnson, E. Jones, CERN Internal Note, 1981.

5. T. Eichten et al., Particle Production in Proton Interactions in Nuclei at 24 GeV/c, Nucl. Phys. B44:333, 1972.

6. C. Hojvat, A. Van Ginneken, Calculations of Antiproton Yields for the Fermilab Antiproton Source, FERMILAB-Pub-82/43, 1982.